PHYSICAL REVIEW A VOLUME 56, NUMBER 6 DECEMBER 1997

Determination of the dipole polarizabilities of $H_2^+(0,0)$ and $D_2^+(0,0)$ by microwave spectroscopy of high-L Rydberg states of H_2 and D_2

P. L. Jacobson, D. S. Fisher, C. W. Fehrenbach, W. G. Sturrus,* and S. R. Lundeen
Department of Physics, Colorado State University, Fort Collins, Colorado 80523

(Received 4 August 1997)

The fine-structure intervals separating $n=9$ and 10, $L=5-8$ Rydberg levels of H_2 and D_2, bound to the $v=0$, $R=0$ ground states of H_2^+ and D_2^+, are measured with microwave spectroscopy and used to determine the isotropic dipole polarizabilities of both ion ground states. The results $\alpha_s(H_2^+)=3.1659(8)a_0^3$ and $\alpha_s(D_2^+)=3.0667(8)a_0^3$ are more precise than existing theoretical predictions, and their explanation will pose a substantial challenge to the theory of this fundamental ion. [S1050-2947(97)51212-1]

PACS number(s): 33.15.Kr, 33.15.Pw, 33.20.Bx

The one-electron molecule H_2^+ provides a unique opportunity for precise calculations of molecular properties, including relativistic and radiative corrections [1]. Unfortunately, it is difficult in practice to calculate most of its properties with accuracy exceeding 0.1%, the level at which the Born-Oppenheimer and adiabatic approximations begin to fail [2,3]. The development of new theoretical techniques, necessary for increased accuracy, is presently hindered by the lack of precise experimental measurements of H_2^+ properties. One method that can be used to determine such properties is precise spectroscopy of the fine structure of nonpenetrating Rydberg states of H_2. In essence, the distant Rydberg electron acts as a sensitive probe of the H_2^+ ion's long-range electric and magnetic properties. Spectroscopy of this type has already been carried out for a number of H_2 Rydberg states bound to $(v=0, R=1)$ states of H_2^+ [4–6]. We report here further measurements for high-L Rydberg levels of both H_2 and D_2 bound to the $(v=0, R=0)$ ground states of the respective molecular ions. These measurements determine the isotropic dipole polarizabilities of both ions with a precision of about 0.03%, sufficient to challenge the best available theory.

High-L Rydberg states of H_2 (or D_2) can be characterized by the quantum numbers describing the free ion core (v,R), the hydrogenic Rydberg electron (n,L), and by the vector sum of the two angular momenta, $\vec{R}+\vec{L}\equiv\vec{N}$. Thus, in general, the fine structure of such Rydberg states consists of $2R+1$ eigenstates for each value of n,L. We denote such vector coupled eigenstates as $(v,R)nL_N$. In the case of $(0,0)nL_L$ levels reported here, the fine structure is very simple, with only a single eigenstate corresponding to each value of n,L. This structure is analogous to the fine structure of high-L Rydberg states of *atomic helium* since the $R=0$ molecular ion cores appear spherically symmetric to the nonpenetrating Rydberg electron.

The electric fine structure of high-L Rydberg states of H_2 and D_2 can be calculated from an effective potential model that eliminates the core electron's degrees of freedom, leaving a single-electron problem in which the core electron's effects are confined to certain parameters in the effective potential, $V_{\rm eff}$ [7,8]. The Rydberg fine structure can be found as a perturbation series in $V_{\rm eff}$:

$$E(v,R,n,L,N)=E^{[0]}(v,R,n)+E^{[1]}(v,R,n,L,N)+E^{[2]}(v,R,n,L,N)+\cdots, \quad (1)$$

where

$$E^{[1]}(v,R,n,L,N)=\langle\psi^0|V_{\rm eff}|\psi^0\rangle \quad (2)$$

and

$$E^{[2]}(v,R,n,L,N)=\sum_{v'R',n',L'}\times\frac{|\langle\psi^0(v,R,n,L,N)|V_{\rm eff}|\psi^0(v',R',n',L',N)\rangle|^2}{E^0(v,R,n)-E^0(v',R',n')}. \quad (3)$$

Generally, this perturbation series and the multipole series implicit in $V_{\rm eff}$ both converge rapidly for high-L Rydberg levels, and increasingly so as L increases. Because of this, it is possible to account for the fine structure with just a few terms of $V_{\rm eff}$ and only $E^{[1]}$ and $E^{[2]}$.

The spin fine structure of high-L H_2 (or D_2) Rydberg states is due to the magnetic interactions between the Rydberg electron and the core electron ($H_{\rm MFS}$) and the hyperfine interactions between the nuclear spins and the core electron spin ($H_{\rm HFS}$) [4]. For $R=0$ Rydberg states, such as those considered here, the only nonzero contribution to hyperfine structure is the scalar term, and since a strict selection rule ($\Delta F_C=0$) prevents transitions between states with different values of the core spin ($\vec{F}_c=\vec{I}+\vec{S}_c$), $H_{\rm HFS}$ makes no direct contribution to transition energies. The spin-orbit and spin-spin energies in $H_{\rm MFS}$ result in $2(2F_c+1)$ spin components spanning a frequency range of a few MHz for the transitions under study here. For $H_2^+(0,0)$, which has $I=0$, these are the same four spin components seen in high-L Rydberg states of atomic helium. For $D_2^+(0,0)$, which can have $I=0$ or 2, this results in 24 spin components spanning approxi-

*Permanent address: Deptartment of Physics, Youngstown State University, Youngstown, OH 44555.

 © 1997 The American Physical Society

mately the same range of frequencies. Exchange energies were determined to be negligible (<0.01 MHz) for the high-L levels studied here.

The intervals measured here were determined using the same general technique used for previous microwave fine-structure studies in H_2 [4]. A fast beam of H_2 (or D_2) Rydberg states was formed by neutralizing an 11-keV beam of H_2^+ (or D_2^+) ions. The population of specific $n=9$ or 10 Rydberg levels, e.g., $(0,0)9K_7$, was monitored using the resonant excitation Stark ionization spectroscopy (RESIS) technique, in which a Doppler-tuned CO_2 laser excites a particular $n=9$ or 10 level to a high-lying discrete level that is subsequently ionized, leading to an excitation-induced ion current proportional to the population of a specific Rydberg level. Three aspects of the experimental technique differed from previous studies [4]. First, the ion beam was neutralized in a Cs-vapor charge-exchange cell, rather than a gas cell, leading to more efficient population of the $n=9$ and 10 Rydberg levels. Second, the preionizer, after neutralization, used two repeated regions of strong field, separated by a region of zero field. This reduced the background signal from highly excited Rydberg levels, including those regenerated after the first ionization field by conversion of vibrational and rotational energy to electronic energy [9]. Last, an improved Rydberg detector was used that increases the collection efficiency for the RESIS signal and reduces the background [10]. Taken together, these three refinements improved the signal-to-noise ratio over previous experiments [4] by a factor of about 15. A report of the RESIS excitation spectra of H_2, D_2, and HD made with this apparatus is in preparation [11].

Microwave transitions between adjacent fine-structure levels were induced in a section of 50Ω transmission line that preceded the laser-excitation region. For example, when the laser is tuned to excite and detect the $(0,0)9K_7$ level, the microwaves might induce transitions to the $(0,0)9I_6$ level which lies about 870 MHz below it, changing the population of the $(0,0)9K_7$ level and, therefore, the detected ion flux. In order to insure a population difference between the coupled levels, an initial CO_2 laser interaction region (tuned to the same excitation as the second) precedes the microwave region and depletes the population of the detected level by about a factor of 2. Similar sequences of transitions were used to observe the I-K and K-L transitions in $n=9$ and 10 and the $10H$-I transition.

A typical measured resonance line shape for the $9I$-K transition is shown in Fig. 1 for both isotopes studied here. The resonance linewidth, controlled by the transit time through the 1-m-long microwave-interaction region, is about 0.8 MHz for D_2 and 1.1 MHz for H_2. As Fig. 1 illustrates, this partially resolves the spin structure of the transition. The smooth curves in Fig. 1 are fits of the measured signals to superpositions of the proper number of spin components whose positions, relative to the spinless interval, are calculated, and whose relative intensities are taken to be proportional to the statistical weight of the lower-J level. The individual spin components are illustrated by the stick diagrams in Fig. 1. These fits determine the spinless line centers with a precision of 0.1 MHz or less.

For each transition and isotope, measurements were made for both directions of propagation of the microwave field

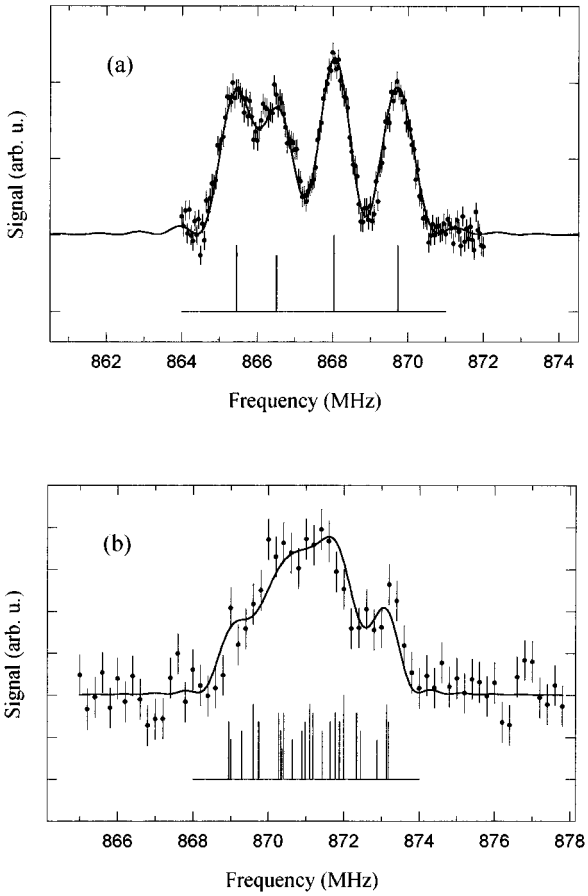

FIG. 1. Resonance line shapes for the $(0,0)9I_6$-$(0,0)9K_7$ transition in (a) H_2 and (b) D_2. The smooth curves are fits incorporating the calculated spin structure, which is shown in the separate stick diagram.

with respect to the molecular beam. Both first- and second-order Doppler shifts are removed by taking the geometric mean of these two results to determine the transition frequency for stationary molecules. The only significant systematic correction is due to the possible presence of stray electric fields within the microwave region, which could Stark shift the resonances. For this study, these fields were measured by periodic observation of the 10^3G_5-10^3H_6 transition in atomic helium using the same apparatus. Since this transition frequency, in zero field, has been measured previously [12], its known Stark shift rate determines the rms stray field and the appropriate small Stark shift corrections (<0.03 MHz) to each measured resonance position. The first column of Table I shows the final results for the ten fine-structure intervals after this correction.

In order to determine the ionic polarizabilities from these results, we take each fine-structure interval to be given by

$$\Delta E_{\mathrm{Tot}}=\Delta E^{[1]}+\Delta E^{[2]}+\Delta E_{\mathrm{rel}}. \tag{4}$$

The last two terms, the spin-independent relativistic correction [4] and the second-order polarization energy, can be calculated and subtracted from the observed fine-structure intervals. Evaluating $\Delta E^{[2]}$ involves computing the energy shift of each level of the transition due to coupling to all other Rydberg states through V_{eff}. This is computed by the

TABLE I. Measured fine-structure intervals and inferred first-order polarization energies for H_2 and D_2 (all results in MHz).

		H_2		
Interval	$\Delta E^{\rm obs}$	$\Delta E_{\rm rel}$	$\Delta E^{[2]}$	$\Delta E^{[1]}$
$9I$-$9K$	864.563(5)	4.93	4.14(22)	855.49(22)
$9K$-$9L$	370.696(16)	3.77	3.81(4)	363.12(4)
$10H$-$10I$	1 659.180(5)	4.90	−33.1(14)	1687.4(14)
$10I$-$10K$	630.795(15)	3.59	−12.10(18)	639.31(18)
$10K$-$10L$	274.072(20)	2.75	−2.51(3)	273.83(4)
		D_2		
Interval	$\Delta E^{\rm obs}$	$\Delta E_{\rm rel}$	$\Delta E^{[2]}$	$\Delta E^{[1]}$
$9I$-$9K$	873.27(5)	4.93	37.82(21)	830.52(22)
$9K$-$9L$	359.58(7)	3.77	3.99(4)	351.82(8)
$10H$-$10I$	1 687.67(8)	4.90	44.5(13)	1 638.3(13)
$10I$-$10K$	638.01(4)	3.59	14.72(17)	619.70(17)
$10K$-$10L$	273.07(7)	2.75	4.84(3)	265.48(8)

methods described in Ref. [8], including all terms with $s \leqslant 8$. The quoted error bar is derived from the convergence of the multipole expansion. The resulting values of $\Delta E^{[1]}$ are shown in Table I [13].

In order to determine the dipole polarizabilities from the first-order polarization energy intervals, $\Delta E^{[1]}$, we use the prediction that [4]

$$E^{[1]}[(0,0)nL_L] = B_4\langle r^{-4}\rangle_{nL} + B_6\langle r^{-6}\rangle_{nL} + B_7\langle r^{-7}\rangle_{nL}\,, \tag{5}$$

where

$$B_4 = -(1+\varepsilon)^2\frac{\alpha_s}{2},$$

with

$$\varepsilon = \frac{m_e}{2m_N + m_e}, \quad B_6 = -\frac{C_0}{10} + \frac{3\beta_s}{2}. \tag{6}$$

The scalar dipole polarizability α_s is the property of the ion core that we wish to determine. The nuclear-mass-dependent coefficient in B_4 is a kinematic correction that is discussed in Ref. [4]. The scalar quadrupole polarizability C_0 and the scalar nonadiabatic dipole polarizability β_s, have both been calculated [14]. Appropriate averages over vibrational wave functions lead to the predicted coefficients, $B_6 = 7.82$ a.u. for H_2^+ and $B_6 = 7.25$ a.u. for D_2^+. Some, but not all of the coefficients contributing to B_7 have been calculated [4]. In a previous study of Rydberg states bound to $H_2^+(0,1)$, both coefficients were estimated by a fit of data from I-K, H-I, and G-H intervals in $n = 10$ Rydberg levels with the results $B_6 = 8.4(8)$ and $B_7 = -21(6)$. This confirms the theoretical estimates of B_6 to a precision of 10% and gives an experimental estimate of B_7.

In order to determine the best values of α_s for both ions, we compute the radial expectation values [15] and the difference of the expectation values for adjacent values of L.

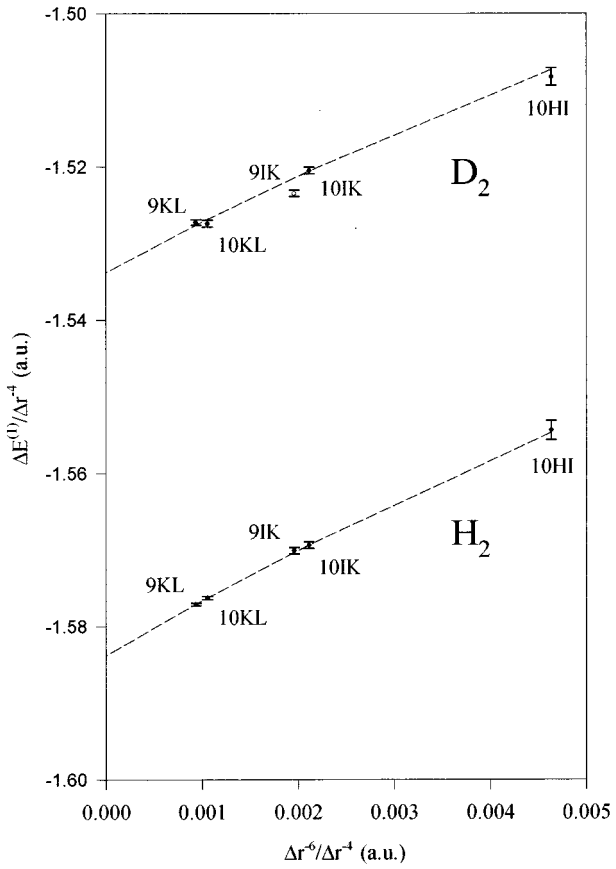

FIG. 2. Scaled transition energies in H_2 and D_2. As described in the text, the y intercepts of the fitted curves (dashed lines) determine the ion polarizabilities. The unfilled point was not used in the fit.

These values are then used to scale the inferred $\Delta E^{[1]}$ (from Table I) in order to form a quantity that is approximately constant:

$$\frac{\Delta E^{[1]}}{\Delta\langle r^{-4}\rangle} = B_4 + B_6\frac{\Delta\langle r^{-6}\rangle}{\Delta\langle r^{-4}\rangle} + B_7\frac{\Delta\langle r^{-7}\rangle}{\Delta\langle r^{-4}\rangle}. \tag{7}$$

Figure 2 shows a plot of these scaled intervals vs the coefficient of B_6 in Eq. (10). If B_7 were zero, this should result in a linear plot, whose intercept is simply related to the polarizability α_s. There are clearly two lines in Fig. 2, indicating that the polarizabilities are significantly different for H_2^+ and D_2^+. The slopes of the two lines appear to be similar. As discussed above, they are expected to be in the ratio 0.927, the ratio of the B_6's for the two isotopes. Similarly, the curvature of the two lines, which is represented by the coefficient B_7, is expected to be very similar for the two ions. The previous experimental estimate of B_7 for $H_2^+(0,1)$, $B_7 = -21(6)$ a.u., is more precise than can be obtained from the data reported here, since the curvature is much more significant for the $10G$-H interval reported in Ref. [4]. We therefore adopt that estimate for B_7, fix the ratio of the coefficients B_6 for the two ions to be 0.927 as estimated theoretically, and fit the data of Fig. 2 for one slope and the two intercepts. This fit is illustrated by the dashed curve in Fig. 2. One point, the one derived from the D_2 $9I$-K interval,

TABLE II. Measured and calculated polarizabilities for H_2^+ and D_2^+ (results in a_0^3).

Ion	Experiment	Theory	$(E-T)/E$	$(E-T)/\sigma$
$H_2^+(0,1)$	3.177 0(34)[a]	3.180 9[b]	−0.12(11)%	−1.1
$H_2^+(0,0)$	3.165 9(8)	3.171 3[b]	−0.171(24)%	−7.1
$D_2^+(0,0)$	3.066 7(8)	3.073 1[c]	−0.209(27)%	−7.8

[a]Reference [4].
[b]Reference [17].
[c]Reference [18].

differs significantly (by 5σ) from the fit, and so we choose to exclude it [16]. The fit to the remaining nine points is good, with a χ^2 of 3.6 for 6 degrees of freedom. The fitted value of B_6 for H_2 is 7.8(5), in agreement with the theoretical estimate.

The fitted intercepts B_4 determine the polarizabilities according to Eq. (6). The results, shown in Table II, represent the first determination of a D_2^+ polarizability and only the second determination for H_2^+. Table II compares the measured results for these three molecular ions to calculated polarizabilities [17,18], based on the standard ''clamped nucleus'' approximation. In this approach, the polarizabilities are calculated as a function of internuclear separation in a body-fixed coordinate system, and then averaged over the internuclear separation distribution in a rovibrational wave function calculated for an adiabatic internuclear potential. All three comparisons show the experimental value to be smaller than the calculated value by about 0.2%. This represents very good agreement, given the approximations inherent in the calculation, but it also clearly points to the need for better theoretical methods. A more precise calculation will require both a more accurate expression for the polarizability [19] and the consistent inclusion of nonadiabatic corrections to the H_2^+ wave function [3]. Finally, we note that of the two ions, D_2^+ shows the larger discrepancy with theory, contrary to what one might expect, because of its larger nuclear mass.

Further improvements in experimental precision will be important for testing improved calculations. Some improvement may be anticipated by extending the pattern of experimental data to include a wider range of L levels and similar fine-structure intervals in $n=11$. It should be noted, however, that even the present result is not solely limited by experimental precision. Derivation of the polarizabilities from the measured intervals depends critically on the calculation of the second-order polarization energies $\Delta E^{[2]}$, and any improvements in those calculations could increase the precision of the conclusions. In addition, improved estimates of the higher-order H_2^+ polarization terms, especially the uncalculated nonadiabatic terms in $V_{\rm eff}$ proportional to r^{-7}, would increase confidence in the analysis. Finally, it may eventually be possible to find alternative approaches to calculating the fine structure of high-L H_2 Rydberg levels that avoid the perturbative expansion in $V_{\rm eff}$ and provide a more precise connection between the measured fine-structure intervals and the core polarizabilities.

This work was supported by the National Science Foundation through Grant No. PHY95-07533.

[1] Alan Carrington, Iain R. McNab, and Christine M. Montgomerie, J. Phys. B **22**, 3551 (1989).
[2] David M. Bishop, Phys. Rev. Lett. **62**, 3008 (1989).
[3] James F. Babb and A. Dalgarno, Phys. Rev. Lett. **66**, 880 (1991).
[4] W. G. Sturrus, E. A. Hessels, P. W. Arcuni, and S. R. Lundeen, Phys. Rev. A **44**, 3032 (1991).
[5] Z. W. Fu, E. A. Hessels, and S. R. Lundeen, Phys. Rev. A **46**, R5313 (1992).
[6] P. W. Arcuni, Z. W. Fu, and S. R. Lundeen, Phys. Rev. A **42**, 6950 (1990).
[7] W. G. Sturrus, E. A. Hessels, P. W. Arcuni, and S. R. Lundeen, Phys. Rev. A **38**, 135 (1988).
[8] P. W. Arcuni, E. A. Hessels, and S. R. Lundeen, Phys. Rev. A **41**, 3648 (1990).
[9] T. J. Morgan, C. F. Barnett, J. A. Ray, and A. Russek, Phys. Rev. A **20**, 1062 (1979).
[10] D. S. Fisher *et al.* (unpublished).
[11] P. L. Jacobson *et al.* (unpublished).
[12] E. A. Hessels, P. W. Arcuni, F. J. Deck, and S. R. Lundeen, Phys. Rev. A **46**, 2622 (1992).
[13] Equation (7) omits the effects of Casimir forces, predicted for these states by James F. Babb and Larry Spruch, Phys. Rev. A **50**, 3845 (1994), since they are too small to affect the analysis.
[14] David M. Bishop and Lap M. Cheung, J. Phys. B **11**, 3133 (1978) (the coefficient β_s is equal to the isotropic average of the S_{-3} moment function, as discussed in Ref. [5]); **12**, 3135 (1979) (the coefficient $C_0=C_{ZZZZ}+8C_{XZXZ}+8C_{XXXX}$).
[15] K. Bockasten, Phys. Rev. A **9**, 1087 (1974). The appropriate core mass dependence of the radial expectation values can be obtained by replacing the Bohr radius a_0 by $(1+m_e/M_I)a_0$, where M_I is the mass of the H_2^+ or D_2^+ ion and m_e is the electron mass.
[16] We have no reason to doubt the measured interval, but suspect that the calculated $E^{[2]}$ correction may be unreliable due to a chance coincidence with perturbing levels. In any event, including this point in the fit only worsens the fit without changing the intercepts by more than the quoted errors.
[17] David M. Bishop and Brenda Lam, Chem. Phys. **65**, 679 (1988).
[18] James F. Babb (private communication).
[19] David Bishop, Lap M. Cheung, and A. D. Buckingham, Mol. Phys. **41**, 1225 (1980).